CO$_2$ Reduction Reactions by Rhodium-Based Catalysts

Danilo Bonincontro and Elsje Alessandra Quadrelli

Abstract Reduction reactions of CO$_2$ using chemicals obtained from renewable energy sources (as for example, dihydrogen obtained using renewable-issued electricity) or using directly renewable energy sources can contribute to store and use renewable energies in our current infrastructures. Rh-based catalysts have been playing a key role in the field of CO$_2$ reduction. From its very first application as homogeneous catalyst to now, several Rh-based catalytic systems have been successfully tested. This chapter gives the reader an overview as well as a mechanistic insight where possible into the Rh-catalysed CO$_2$ reduction reductions: production of formic acid and higher carboxylic acids with homogeneous catalysts, methane, CO and various oxygenated compounds via heterogeneous catalysis, and various products by means of electro- and photocatalysis.

Keywords Carbon dioxide • Electrocatalysis • Formic acid • Heterogeneous catalysis • Homogenous catalysis • Mechanism • Photocatalysis • Rhodium

Contents

D. Bonincontro
Université de Lyon, C2P2, UMR 5265, CNRS – Univeristé de Lyon1 UCBL – CPE Lyon, 43 Bvd du 11 Novembre 1918, 69616 Villeurbanne, France

Dipartimento di Chimica Industriale "Toso Montanari", Viale Risorgimento 4, Bologna, Italy

E.A. Quadrelli (✉)
Université de Lyon, C2P2, UMR 5265, CNRS – Univeristé de Lyon1 UCBL – CPE Lyon, 43 Bvd du 11 Novembre 1918, 69616 Villeurbanne, France
e-mail: quadrelli@cpe.fr

1   Introduction

Carbon dioxide emissions are emerging as a towering side effect of fossil fuel utilization. As a major energy provider, accounting for 81% of our 2013 global consumption, fossil fuels are responsible for a big share of the year's – 31.6 GT of CO_2 emissions [1, 2]. Despite considerable efforts to reduce such consumption and curb CO_2 emissions, the predicted increase in overall energy consumption, and the expected continued dominance of fossil fuels in the energy mix for the next decades, explains in part why, regardless the scenario envisaged [3], CO_2 emissions are expected to raise continuously for at least the next decade (see Fig. 1) [2]. Albeit nature provides very efficient carbon cycles, capable mainly through photosynthesis and ocean capture to absorb back about half of the anthropogenic emissions [4], the CO_2 buildup cannot be curbed unless major dedicated efforts are directed to this aim [5–11].

   Carbon dioxide has long been considered an intractable waste, due, inter alia, to its very high thermodynamic stability. The rare – yet very established and industrially relevant – applications of carbon dioxide utilization, production of urea to
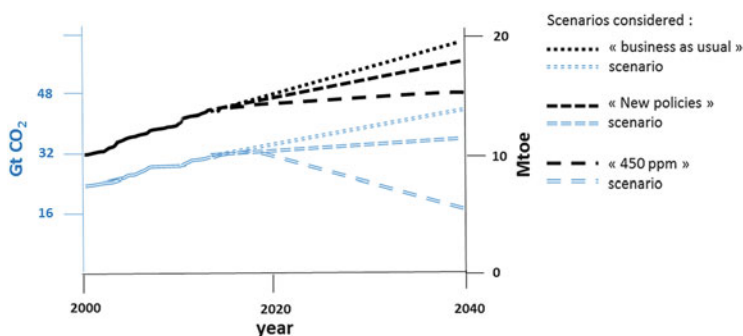

Fig. 1 World energy demand (*right axis* and *black lines*) and CO_2 anthropogenic emissions (*left axis* and *blue lines*) between 2000 and 2040 measured and forecasted according to different scenarios: the "business-as-usual" scenario (i.e., no dedicated change in energy policy), the "new policies" scenario which takes into account the environmental pledges announced by the countries in October 2015 before the COP21, and the "450 scenario ppm" (officially named Scenario 450) developed with the goal to maintain the greenhouse gases concentration in atmosphere under 450 ppm of CO_2 [2]

name one, typically do not change the carbon oxidation number or at least do not require large energy input due to the favorable thermodynamic parameters of the carbonation reactions [5–8]. The capacity to synthesize from CO$_2$ sufficiently long-lived materials (ex polymers or building blocks from carbionation of waste) are some of the examples that show how carbon dioxide utilization (CDU) reactions are emerging as an important complement/alternative to carbon capture storage [5–8].

At the opposite end of such carboxylation reactions, reactions aiming at breaking (and hence reducing) one of these very stable C=O bonds imply substantial energy supply (see Scheme 1). CO$_2$ thermodynamic stability explains the need for very large quantities of energies to jolt the carbon atom back into a reduced valence state and thus removing one C=O bond and/or forming new C–C or C–H bonds such as in CO, HCOOH (+II oxidation number), CH$_3$OH (−II oxidation number) or CH$_4$ (−IV). This energetic hurdle has made CO$_2$ unattractive for reduction reactions until recently. Now, with the overarching desire to find ways to store renewable energy as chemical energy, this very same thermodynamic stability makes CO$_2$ a suitable molecule to store energy. Indeed, CO$_2$ is asserting itself as a crucial vector molecule for the injection of renewable energy in our current infrastructure thus providing a key technology for avoidance of fossil fuel [9, 10]. This review will focus on these CO$_2$ reduction reactions.

In the chemical industry, over 90% of the processes involve at least one catalytic step [11]. Catalysis plays a similar fundamental role in the chemistry enabling the reduction of CO$_2$ in added-value products [5–10]. Among the several catalytic systems, we will here review the role of rhodium-based catalysts in the CO$_2$ reduction reactions.
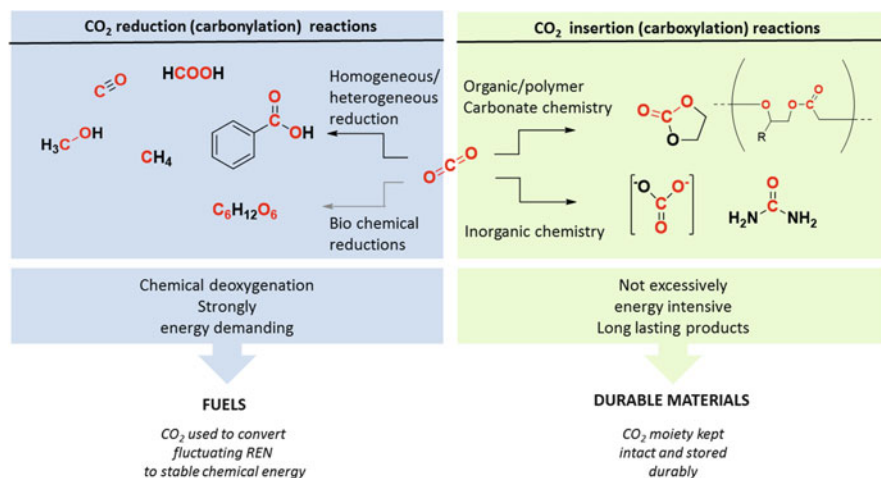
Scheme 1 Overview of two major types of CDU reactions: *left*, reduction reactions as mean to provide an energy vector for fossil fuel avoidance, see text; *right*, in CO$_2$ insertion reaction as mean to chemical storage of CO$_2$ molecules

2 Molecular Catalysts

2.1 *Formic Acid*

World formic acid (FA) production was 950,000 t in 2014, and its industrial applications are very wide, ranging from silage manufacturing, leather and tanning production, to pharmaceutical industry [12]. More than 80% of FA world production comes from the hydrolysis of methyl formate which is obtained through the reaction between CO and methanol (which is recycled after the hydrolysis). A more sustainable approach for its production could become the direct reduction of CO_2 with H_2 produced with renewable energy, r-H_2 (see Scheme 2) [10, 13].

To estimate the impact of such potential technology switch, one could first propose the following upper boundary: replacing the entire traditional production with CO_2-based technologies could lead to a consumption of 1 Mt y^{-1} of CO_2 (around 0.003% of the overall annual CO_2 emission). At the same time, this estimate does not take into account the major role that CO_2-based formic acid production could make: store and transport hydrogen through the cycle reported in Scheme 2 [5–9, 13–15]. Such approach is claimed to be CO_2-emission neutral if the dihydrogen is "renewable" hydrogen, r-H_2, and permits easier and safer transportability of liquid fuel with respect to compressed molecular hydrogen. In this case of formic acid formation (Eq. 2), the role of CO_2 reaction would not be about storing (or consuming) CO_2, but rather about avoiding later CO_2 emissions through fossil fuel replacement with renewable energy (REN)-based fuels (see column 1, Scheme 1). In this latter case, the volume of formic acid produced from CO_2 depends on the penetration of such energy vector in the infrastructures, which, if successful, could largely overpass the figures cited above.

The first work which showed CO_2 reduction into formic acid following Eq. (2) was through rhodium-based catalysis into the spotlight. Inoue reported in 1976 that $RhCl(PPh)_3$ was among the best catalysts to achieve formic acid production directly from CO_2 and H_2 [16]. The screening of different transition metal complexes was performed in nonaqueous medium (benzene) and in the presence of a base and water (typical molar ratio base/water 1/10). Among the different complexes tested, the Wilkinson's complex, $RhCl(PPh)_3$, in the presence of trimethylamine as base was found active, second only to ruthenium-based system. A deep insight into the catalytic behavior of Wilkinson's complex was reported by

Scheme 2 Reaction scheme for current industrial route to formic acid (Eq. 1) and alternative route directly from CO_2 (Eq. 2), which is part the proposed CO_2-mediated storage and release of H_2 [10, 13–15]
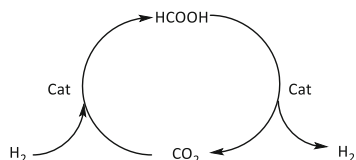
Ezhova [17]. This work highlighted the effect of different parameters on the catalytic behavior of the complex. A predominant role is played by the solvent: heptane, benzene, and THF were found to repress the activity of the complex, while DMSO and MeOH have been found to be suitable solvents for this reaction, even though when MeOH is used the presence of methyl formate is detected at the end of the reaction. The study of the catalytic properties of other Rh(I)-containing species demonstrated the importance of phosphine ligands: all complexes containing a phosphine ligand were found to be active in the conversion of CO$_2$ into formic acid; on the other hand, the complex without a phosphine ligand are inactive, and some of them showed activity only after the addition of phosphine ligands. The ^{31}P-NMR study reported in the same paper suggested that RhCl(PPh$_3$)$_2$(NEt$_3$) is the precursor of the active complex, and its decomposition is inhibited by the excess of phosphine.

The conversion of CO$_2$ in nonaqueous solvents is also catalyzed by RhH (diphosphine) complexes [18]. The diphosphines are prepared in situ using the bidentate phosphine 1,4-bis(diphenylphosphino)butane (dppb, Ph$_2$P-(CH$_2$)$_4$-PPh$_2$) and two different Rh-containing precursors: [RhCl(cod)$_2$]$_2$ and [RhH(cod)$_4$] (cod = 1,5-cyclooctadiene). The first system suffers from an "induction time" that could be overcome by an activation with H$_2$ or HCOOH, which is necessary to obtain RhH(dppb), the postulated active species. In order to understand which of the effects are structural changes in phosphine ligands on the catalytic activity of Rh (I) precursors, Leitner's group synthesized and tested the catalytic activity of a series of [(P$_2$)Rh(hfacac)] (hfacac = 1,1,1,5,5,5-hexafluoroacetylacetonate) complexes. It was found that the larger the P-Rh-P bite angle, the greater the ^{103}Rh NMR chemical shift and the higher the reaction rate [19]. Further studies were focused on the determination of the accessible molecular surface (AMS) [20] of such complexes and their correlation with the activity, and it was found that the AMS inversely correlated with the reaction rate.

In order to obtain water-soluble Rh(I)-based complexes, the already mentioned [RhCl(cod)$_2$]$_2$ and [RhH(cod)$_4$] precursors were modified using the water-soluble sodium trisulfonated triphenylphosphine ligand (C$_6$H$_4$-m-SO$_3^-$Na$^+$)$_3$P, TPPTS) in a ratio P:Rh = 2.6:1 [21]. Both complexes were found active in the reduction of CO$_2$ into selective formic acid using NEt$_3$ as base. The complex RhCl(TPPTS)$_3$ was also successfully tested. Amine variation sensibly affected the catalytic performances. NEt$_3$ and HNEt$_2$ showed the best performances, while ethanolamines reduced the catalytic activity. The base is indeed believed to play a crucial role in the catalytic cycle, since monohydridorhodium complex, RhH(TPPTS)$_3$L, is formed only in the presence of a base (see Scheme 3).

All the catalytic cycles reported so far involve CO$_2$ insertion into Rh(I)–H bonds. A DFT calculation showed that the energy associated to the CO$_2$ insertion into the Rh–H bond is higher for Rh(III) than for Rh(I) [23]. This different behavior could explain why Rh(III)-containing complexes are not commonly used. However, as it will be discussed in Sect. 4, a Rh(III) complex were found to be active as an electrocatalyst in the conversion of CO$_2$ into formate.

A recent development in the field of formic acid production with rhodium-based catalysts in the context of carbon capture and utilization (CCU) was proposed by Li
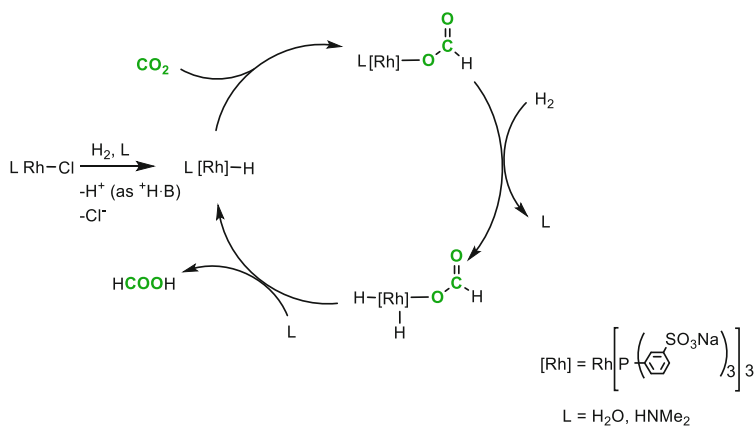
Scheme 3 Catalytic cycle for CO_2 conversion into formic acid catalyzed by $ClRh(TPPTS)_3L$ in the presence of a base, B (e.g., NEt_3 $HNEt_2$, ethanolamine) [22]
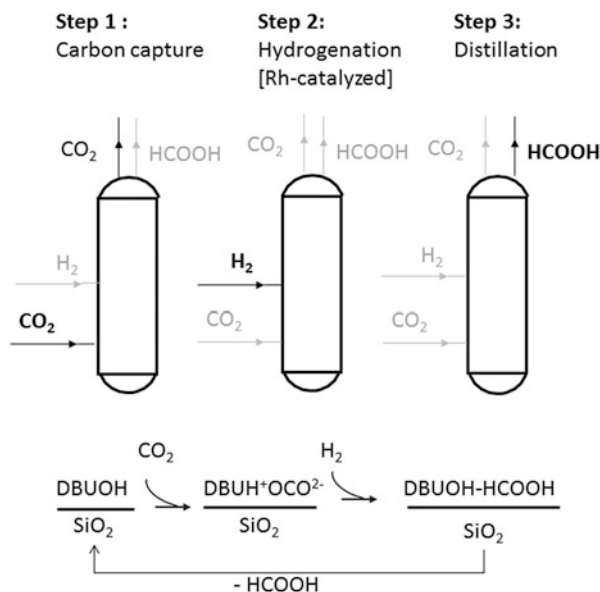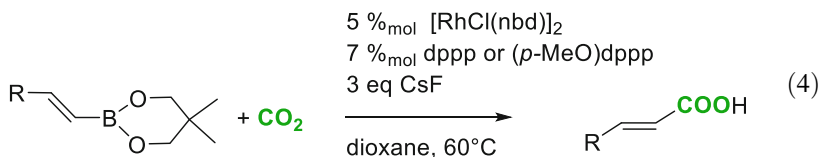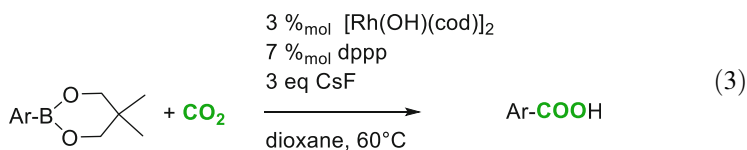

Fig. 2 Proposed CCU process for the conversion of CO_2 into formic acid mediated by silica-supported DBU and Rh-based catalyst [24]

[24] with an integrated carbon capture and utilization (CCU) process for the in situ conversion of CO_2 into formate. According to the authors, 99% of the CO_2 captured can be converted into formate using suitable amidine derivative 1,8-diazabicyclo [5.4.0]-undec-7-ene (DBU) as CO_2 capturing agent and $RhCl_3$ as catalyst precursor. The immobilization of the amidine derivative over silica gave rise to the formation of solid capturing agent which was equally found to be effective in the process. Such solid could be regenerated yielding a three-step chemical process (see Fig. 2).

In summary, formic acid has been one of the first catalytic targets of Rh-based CO$_2$ conversion and has continued to attract considerable interest in the context of coupling with CO$_2$ capture but also to other longer carbon chain targets (see below).

2.2 Higher Carboxylic Acids

An attractive target for the CO$_2$ conversion is the production of carboxylic acids, which are very widely used chemicals [5–8]. The use of CO$_2$ as electrophile reagent in the carboxylation reaction requires high nucleophile reactants, such as organolithiums or Grignard reagents. Alongside these classical approaches, different catalytic cycles involving transition metal complexes have been developed, among which are Rh(I) species [25]. For example, [Rh(OH)(cod)]$_2$ was found to be an effective precursor in the carboxylation of the ester of a wide range of arylboronic acid under mild conditions (1 atm of CO$_2$ at 60°C in dioxane as solvent in the presence of 1,3-bis(diphenylphosphino)propane, dppp, see Eq. 3) [26], which makes this reaction particularly useful when the Grignard reagent route is not available. The analogous precursor [RhCl(nbd)]$_2$ (nbd = norbonadiene) was used in the carboxylation of alkenylboronic acids in the already mentioned operative conditions (Eq. 4).

$$\text{Ar-B}\underset{\text{O}}{\overset{\text{O}}{\diagdown}}\!\!\diagup + \text{CO}_2 \quad \xrightarrow[\text{dioxane, 60°C}]{\substack{3\ \%_{\text{mol}}\ [\text{Rh(OH)(cod)}]_2 \\ 7\ \%_{\text{mol}}\ \text{dppp} \\ 3\ \text{eq CsF}}} \quad \text{Ar-COOH} \qquad (3)$$

$$\text{R}\diagdown\!\!=\!\!\diagup\text{B}\underset{\text{O}}{\overset{\text{O}}{\diagdown}}\!\!\diagup + \text{CO}_2 \quad \xrightarrow[\text{dioxane, 60°C}]{\substack{5\ \%_{\text{mol}}\ [\text{RhCl(nbd)}]_2 \\ 7\ \%_{\text{mol}}\ \text{dppp or (}p\text{-MeO)dppp} \\ 3\ \text{eq CsF}}} \quad \text{R}\diagdown\!\!=\!\!\diagup\text{COOH} \qquad (4)$$

The rhodium (I) complex [RhCl(cyclooctene)$_2$]$_2$, activated in situ by an alkylating agent such as AlMe$_2$(OMe) and in the presence of tricyclohexylphosphine, PCy$_3$, catalyzes the direct carboxylation of phenylpiridines and phenylpyrazoles (see Eq. 5) [27]. In the proposed catalytic cycle, the Rh(I) catalyst activates the C–H bond; then, after methane reductive elimination from the resulting Rh(III) aryl intermediates, the complex undergoes the nucleophilic insertion of the CO$_2$ moiety in the Rh^I–Ar bond; the final transmetallation step with the aluminum alkylating agent releases the carboxylated species regenerating the active catalytic species (see Scheme 4). The direct carboxylation of benzene and its derivatives (toluene, xylenes, and others) could also be achieved using 1,2-bis(dicyclohexylphosphino) ethane–rhodium(I) chloride complex as precursor [28]. The catalytic cycle proposed for such reaction is the same as the one showed in Scheme 4, and kinetic

$$\text{(5)}$$
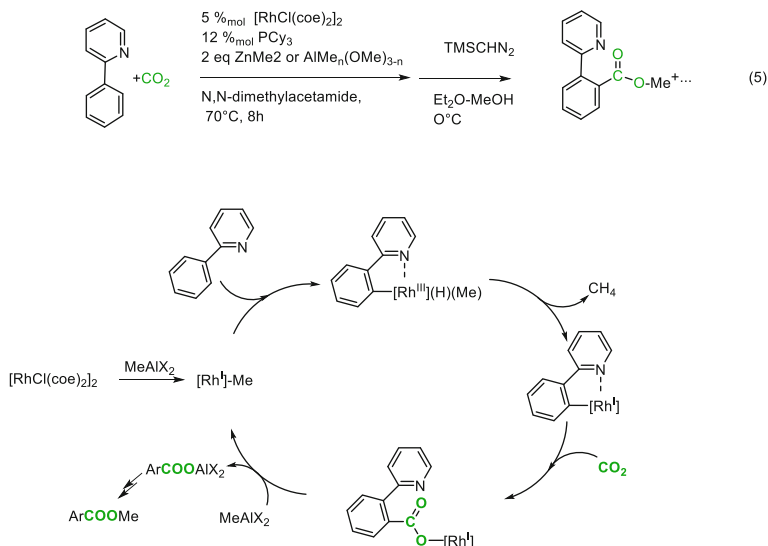
Scheme 4 Proposed catalytic cycle for the carboxylation of phenylpyridine using $[RhCl(coe)_2]_2$ as precursor and PCy_3 as ligand [27]

$$\text{(6)}$$
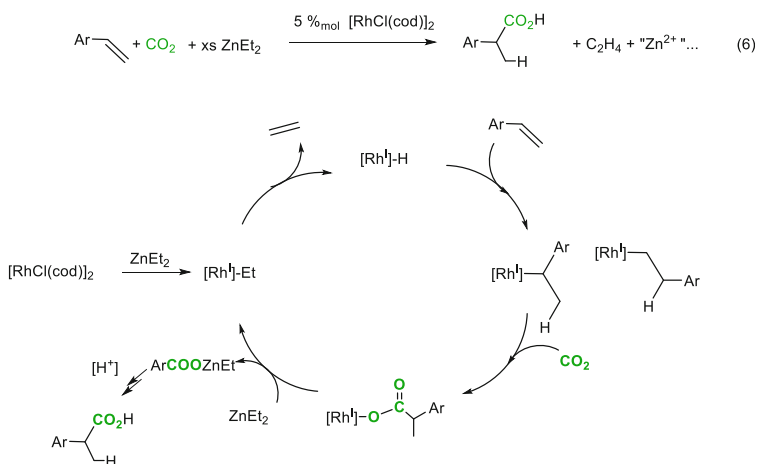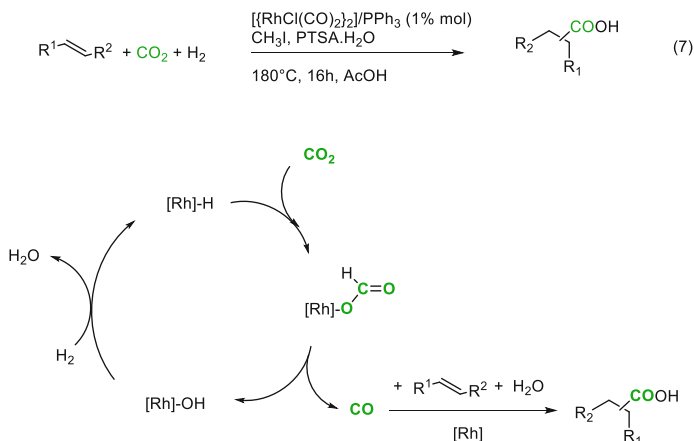
Scheme 5 Rh-catalyzed ($[RhCl(cod)]_2$ as precursor) olefin carboxylation pathway [29]

isotopic labeling experiments suggested that the rate determining step is the C–H bond activation.

Following a proposed reaction mechanism related to the previous one (Scheme 5), the bimetallic system combining catalytic $[RhCl(cod)]_2$ and stoichiometric $ZnEt_2$ achieves hydrocarboxylation of aryl olefins with carbon dioxide (see Eq. 6) [29].

A markedly different mechanistic route was assessed for $[RhCl(CO)_2]_2$-catalyzed hydrocarboxylation of linear and cyclic olefins with CO_2 and H_2 (Eq. 7) in the

$$R^1 \diagdown R^2 + CO_2 + H_2 \xrightarrow[\text{180°C, 16h, AcOH}]{\substack{[\{RhCl(CO)_2\}_2]/PPh_3 \ (1\% \ mol) \\ CH_3I, \ PTSA.H_2O}} R_2 \diagdown \overset{COOH}{\underset{R_1}{\diagdown}} \qquad (7)$$

Scheme 6 Hydrocarboxylation reaction of olefin with CO_2 and H_2, and underpinning catalytic cycles: r-WGS and hydroxycarbonylation reactions [30]
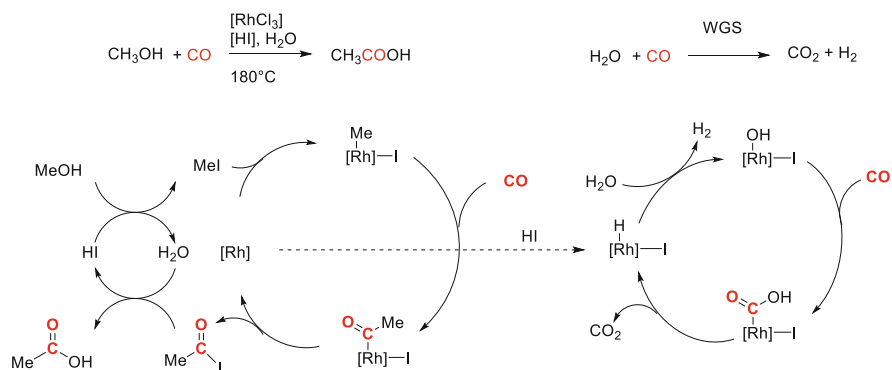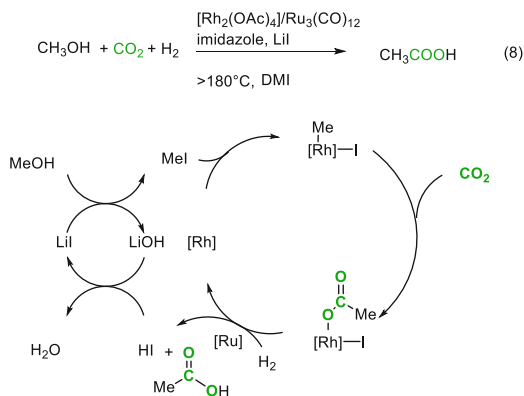

Scheme 7 Catalytic cycles involved in Monsanto acetic acid production by Rh/iodide-based system: *left*, methanol carbonylation; *right*, water-gas shift (WGS) cycle

presence of methyl iodide as promoter in acid conditions (see Scheme 6) [30]. Unlike the aforementioned proposed direct carboxylation routes, the detailed mechanistic studies showed that, in this case at least, the CO_2 is not directly incorporated in the substrate. Robust isotopic labeling studies showed that the products of Eq. (6) are obtained through an intermediary reverse water-gas shift reaction (*r*-WGSR), which acts as the "upstream" cycle for the subsequent hydroxycarbonylation mechanism which involves CO and water as reactants.

The two-cycle mechanism reported in Scheme 6 relies on the catalytic competence of Rh complexes to promote water-gas shift reaction (WGS). Such behavior is in line with the well-established reactivity of the industrial Monsanto catalyst [Rh (CO)₂I₂]⁻, which, beside catalyzing the carbonylation of methanol (its primary goal), can serve as entry point to water-gas shift activities (see Scheme 7) necessary to rhodium solubilization in the reaction media [31, 32].

**Scheme 8** Direct acid acetic production from methanol, CO_2 and H_2 using a Ru/Rh catalytic couple

$$CH_3OH + CO_2 + H_2 \xrightarrow[>180°C, \text{DMI}]{\substack{[Rh_2(OAc)_4]/Ru_3(CO)_{12} \\ \text{imidazole, LiI}}} CH_3COOH \qquad (8)$$

A Ru–Rh bimetallic catalyst, obtained from $Ru_3(CO)_{12}$ and $Rh_2(OAc)_4$ in the presence of LiI and imidazole ligand, seems to bypass such rWGS activity and converts methanol to acetic acid with CO_2 and H_2 (Eq. 8) via a proposed direct hydrocarboxylation route (see Scheme 8) [33]. The proposed cycles involve indeed a direct CO_2 insertion in the Rh–Me bond and subsequent ruthenium-catalyzed hydrogenation of the ensuing Rh-carboxylate. The roles of Rh-/Ru-based catalysts are to be assessed also in view of the reported Ru-only hydroformylation/reduction of alkenes, the hydroxymethylation reaction or the alkoxycarbonylation [34], and the WGS (and *r*-WGS) ability of Rh centers [30–32].

Regardless of these mechanistic considerations, this capacity of CO_2 to act as a CO surrogate (either as an existing intermediate product of the process of just formally) is emerging as a very timely and productive field, where Rh, alongside Ru, appears to play a crucial catalytic role [30, 34].

3 Heterogeneous Catalysts

3.1 Methanation

The CO_2 conversion into methane (known as Sabatier reaction; see Eq. 9) is a well-known route for the CO_2 reduction and can be an attractive way to produce substitute natural gas [8].

$$CO_2 + 4H_2 \rightleftarrows CH_4 + 2H_2O \qquad (9)$$
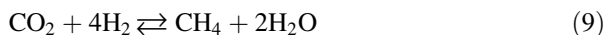
Supported metals are well-known catalysts for the methanation of CO_2 [35–40], and these included Rh-based catalysts supported over metal oxides such as γ-Al_2O_3 [37–39] and TiO_2 [37, 40].

Rhodium supported over γ-Al$_2$O$_3$ has been reported to be an active catalyst for the transformation of CO$_2$ into methane even in mild condition (room temperature and atmospheric pressure) [38], although CO$_2$ conversion increases with temperature [41]. In order to obtain a catalytic active species, the catalyst must be reduced with H$_2$ before the reaction [41], and this reduction leads to an increase of Rh(0) species present over the surface as measured by XPS technique [39]. Mechanistically, DRIFTS analysis [39] showed that CO$_2$ is dissociated into CO and O over the Rh surface; this process leads to the formation of two different C-containing species bonded over the catalyst surface: Rh(I)–(CO)$_2$ (also called gem-dicarbonyl species) and Rh(0)-CO. When a pulse of H$_2$ is introduced inside the chamber, the peaks of the gem-dicarbonyl species disappear rapidly; meanwhile, the intensity of the peak related to the mono-carbonyl species does not change. According to this analysis, it appears that the oxidation state of the Rh has a predominant role in the catalytic process. Karelovic and Ruiz [42] prepared and tested different catalysts with different Rh particles and showed that larger particles are more active than smaller ones between 135 and 150°C, while at higher temperature, the reaction rate is independent from the particle size. A similar study was conducted over TiO$_2$-supported Rh catalysts [40]. For metal particles smaller than 7 nm, the rate of methane production increases as metal particles size increases; for bigger particles the rate seems to be independent from the size.

Because of the high cost of the Rh (around 20$/g in 2016) and its lower activity compared to Ni (which suffers from more rapid deactivation than Rh but costs less than 0.01$/g), several attempts to improve the catalytic properties of the Rh/γ-Al$_2$O$_3$ system were proposed by coupling this system with other supported metal species. For instance, the catalytic properties of the Rh(0.3%)/γ-Al$_2$O$_3$ were improved by addition of the (presumably catalytically inactive) Mn (0.5%). Such catalyst showed the same catalytic properties as the Rh(0.5%)/γ-Al$_2$O$_3$ catalyst [43]. The 1:1 mechanical mixture of the inert Pd(5%)/γ-Al$_2$O$_3$ with the active Rh (2%)/γ-Al$_2$O$_3$ possesses higher activity than the Rh-based catalyst alone [44]. This higher activity is thought to be the result of a synergistic effect between the two different catalysts: the hydrogenation of strongly activated carbonyl species adsorbed over Pd surfaces (mostly bridge-bonded CO, at odds with carbonyl hydride species for Rh-only catalyst) is performed by the H species originated by the Rh-containing catalyst. An analogous synergistic effect was found by coupling Rh/γ-Al$_2$O$_3$ and Ni-loaded activated carbon (AC) [45]. In this case, the synergistic effect is due to the high capacity of the Ni/AC system to absorb and activate hydrogen. The migration of such activated hydrogen species to the Rh surface reduces the carbonyl species to methane. At the same time, the hydrogen species keeps the rhodium into a reduced state which is, as already mentioned before, a key feature in the activity of Rh-based system.

Several metal-promoted mesostructured silica nanoparticles (MSN) have been tested [46]. Among these, the Rh-containing one showed the best catalytic activity at 623 K. Differently from the already mentioned metal oxides supports which do not have any role in the mechanism cycle, the MSN support interacts with the

species activated by the metal promoter, leading to the formation of bridged carbonyl, linear carbonyl, and bidentate formate, which are converted into methane.

Rhodium was mentioned among the metals associated with nickel to form "liquid catalyst" for methanation reaction but was not among the most performing co-catalysts [47].

3.2 Dry Reforming

A further reaction in which Rh-containing catalysts are widely used is the CO_2 reforming of methane (also known as methane dry reforming, MDR, Eq. 10) [5–8, 48].

$$CO_2 + CH_4 \rightarrow 2CO + 2H_2 \tag{10}$$
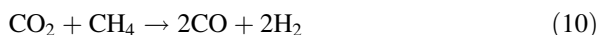
The interest that this reaction has been receiving by the scientific community is justified by the possibility to use this reaction as starting step in the on-site conversion of natural gas into liquid or gaseous fuels through the syngas intermediary [9, 10, 49].

γ-Al_2O_3-supported Rh and Ru were found to be active in the CO_2 reforming of methane [50]. The catalytic tests showed that for reaction temperatures higher than 600°C the Rh-containing catalyst outperforms Ru-based ones in terms of both reactant conversion and deactivation trend. From this first work, different metal oxides have been tested as support for the Rh in order to understand the effect of the interaction between metallic sites and support [51, 52]. Catalytic results showed that irreducible supports (γ-Al_2O_3, La_2O_3, MgO, SiO_2, and Y_2O_3) are more suitable than the reducible ones (CeO_2, Nb_2O_5, Ta_2O_5, TiO_2, and ZrO_2) [52]. Among the former, γ-Al_2O_3, MgO, and La_2O_3 provided stable activities for more than 50 h. The authors suggested that strong interaction between Rh and the support induces high stability of the catalytic system. The lower activity of the catalysts having reducible supports was attributed to the fact that the Rh-metal particles could be partially covered by islets of partially reduced species leading to a decrease of the metal surface area.

The effect of the support in the catalytic performance of Rh-containing catalysts is also significant when Rh is supported with Ni, which is known to have high activity toward the MDR but suffers from severe deactivation due to carbon deposition [53]. Rhodium can limit such carbon deposition [54]. In detail, the bimetallic-loaded boron nitride (BN) showed higher CH_4 conversion and H_2 yield than the analogous γ-Al_2O_3. This enhancement was attributed to the easier formation of Rh–Ni clusters over the BN surface than over γ-Al_2O_3. In fact the metal support affinity is higher for γ-Al_2O_3, and this hinders the formation of such clusters. The synergic effect between Rh and Ni was also found when the two metals were supported over NaY-type zeolite [55].

Rh-containing crystalline materials have been tested in DRM reaction. Hydrotalcite-derived $Rh_1Mg_{71}Al_{28}$ was found to be active in the MDR reaction without any deactivation during 50 h of reaction [56], and the catalyst does not show any change of structure at the end of the reaction. More recent approaches suggested the use of Rh containing pyrochlores [57]. It was showed that replacing Zr by Rh in low amount (2 and 5% wt.) in the lanthanum zirconate pyrochlore structure leads to the formation of catalytic active species. In fact, the catalytic results showed that the unmodified pyrochlore is not able to convert both CO_2 and CH_4; meanwhile, the conversion of both reactants occurs when the two modified pyrochlores are used. Moreover, modified catalysts activity increased during the time: since no preactivation is performed, it was suggested that the reduction of the catalyst is crucial for their activities.

3.3   Oxygenated Compounds

Oxygenated compounds such as ethanol, acetic acid, and oxalate can be obtained from CO_2 using Rh-containing catalysts. The selectivity of CO_2 reduction with H_2 ($H_2/CO_2 = 3$) of Rh/SiO$_2$-based catalyst is strongly affected by the presence of a metal promoter [58]. While unmodified Rh/SiO$_2$ catalyst is highly selective (99.7%) for methane production, the presence of a promoter can induce the formation of oxygenated compounds. A screening of 30 different promoters (in 1:1 Rh/M atomic ratio) showed that four additives (Li, Fe, Sr and Ag) can give rise to rhodium-catalyzed ethanol production. Among these additives, Li is the most selective (15.5%, yield 1.0%). The FT-IR study showed that CO, that comes from the CO_2 dissociation, is adsorbed over the Rh surface as linear and bridged species over the surface of both Li-containing and unpromoted Rh/SiO$_2$ catalyst. Nevertheless, the comparison between the relative intensities of the two peaks for the two different samples showed that over the Li-containing surface, there is a higher amount of bridged species than over the unmodified Rh/SiO$_2$. The authors suggest that the higher amount of CO species could hinder the H_2 adsorption, leading to a lower methane selectivity of the Li-containing catalyst. Higher selectivity (16.0%) and yield (4.3%) could be reached tuning the operative conditions and the metal loading of the Fe-containing Rh/SiO$_2$ catalyst [59].

Ag-modified Rh/SiO$_2$ was found to convert a CO_2/H_2 mixture into different hydrogenated compounds in low yield, since more than 90% of the fed CO_2 is converted into CO. Among the hydrogenated compounds, acetic acid is the most abundant one at 463 K [60]. Using unpromoted Rh/SiO$_2$, Ding [61] proposed a different path to convert CO_2 into acetic acid; it was proposed a stepwise route in which CH_4 is used instead of H_2.

4 Electro- and Photocatalysis

Electrochemical CO_2 reduction is a key technology for the introduction of "green electrons", that is, electricity produced from renewable resources in our current energy infrastructure [62].

Over two decades ago, Rh(III) complexes Cp*RhCl(2,2′-phenanthroline) and *cis*-[Rh(III)(bpy)$_2$(TFMS)$_2$]$^+$ (bpy = 2,2′-bipyridine, TMFS = trifluoromethanesulfonate) were found to be active in the electrochemical conversion of CO_2 into formate [63, 64]. One by-product was molecular hydrogen. The faradaic efficiency in selective CO_2 reduction is generally a key issue: already in one of these first systems [63], the catalytic tests showed that the selectivity in formate decreases as the number of coulomb passed increases, and for hydrogen the trend is the opposite. The authors suggested that the protons required for both formate and hydrogen production come from the tetra-*n*-butylammonium ions of the supporting electrolyte [63].

Another Rh(III)-containing complex that has been successfully tested is [(η^5-Me$_5$Cp$_5$)Rh(bpy)Cl]$^+$ [64]. This work gave the opportunity to have an insight over the mechanism for the electrocatalytic cycle (see Scheme 9).

Beside formate, oxalate can also be obtained from another use in [(RhCp*)$_3$(μ3-S)$_2$]$^{2+}$ electrocatalyzed reduction of CO_2 in the presence of LiBF$_4$, under controlled potential electrolysis at -1.50 V in CO_2-saturated CH$_3$CN [65].

Following short- and medium-term electrocatalysis deployment, photo-based catalysis appears as the necessary (longer-term) next step in the forecast deployment of CDU-based technologies toward more sustainable energy production and resource consumption [8, 62]. Albeit several major technologic forward leaps are
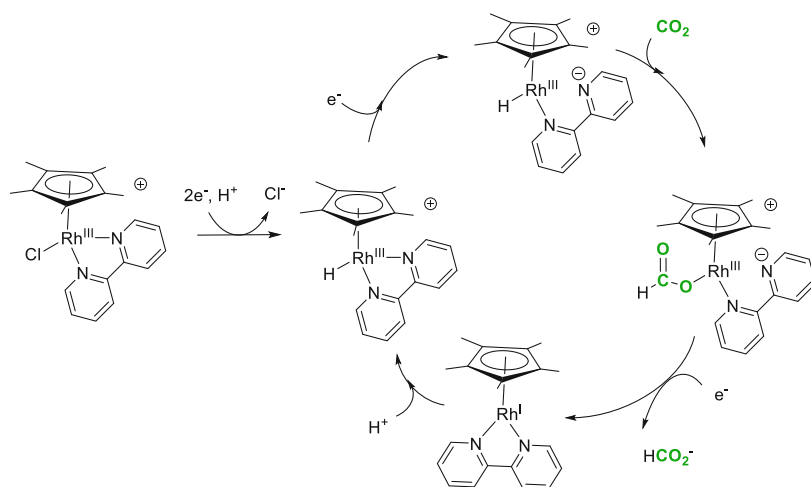

Scheme 9 Electrocatalytic conversion of CO_2 into formate using [(η^5-Me$_5$Cp$_5$)Rh(bpy)Cl]$^+$ as electrocatalyst [64]

necessary to achieve large-scale utilization of photo catalyst, the field already has decade-old precedents as far as Rh-based systems are concerned. The use of Rh-based photocatalysts was firstly disclosed in 1994, when Rasko and Solymosi found that CO_2 photoactivation is stronger over Rh/TiO_2 than over the bare oxide, since the cleavage of a C–O bond was observed only for the test performed over Rh-loaded TiO_2 [66]. Such feature is in agreement with the use of Rh/TiO_2 as catalyst for the CO_2 photo-induced reduction reported the same year [67]. The comparison between TiO_2 and Rh-loaded TiO_2 catalytic behavior in the photore-duction of CO_2 in water showed that the deposition of Rh on TiO_2 leads to an enhancement of the conversion of CO_2 and to a change of the selectivity. In fact when the reaction is performed using pure TiO_2, formic acid and formaldehyde are the only products; using Rh-loaded titania catalysts, methanol was also detected. Eventually, W^{+6}-doped titania and optimized pretreatment, enabled a near-selective production of methanol [67].

The Rh/TiO_2 catalyst was also tested in the gas phase reduction of CO_2 with H_2 [68]. The catalytic results showed that both activity and selectivity strongly depend on the rhodium loading. The 0.5–4% Rh-loading range was investigated, and it was found that low loading of Rh leads to high conversion of CO_2 and high selectivity into CO. On the contrary, high Rh loading suppresses the production of CO, giving rise to a small CH_4 production. The X-Ray absorption spectroscopy (XAS) char-acterization of the different Rh-loaded catalyst showed that rhodium oxidation state depends on the metal amount: the higher the metal amount the higher the Rh-metal/Rh-oxide ratio. Comparing the catalytic results and XAS experiments, it was stated that more the Rh is reduced, the higher the CH_4 selectivity. It was also seen that this catalyst is mildly affected by deactivation. This slow deactivation was firstly ascribed to the formation of rhodium carbonyl compounds, but further studies [69] disproved this hypothesis, since no carbonylic species were detected by IR tests. Hence, it was suggested that the deactivation is due to the CO reduction into CH_x species, which stay over the Rh/TiO_2 and could be not detected by IR means.

Recently, it was found that the use of light-harvesting complexes (LHC) enhance the catalytic activity of Rh-doped TiO_2 in the aqueous phase reduction of CO_2 [70]. In fact, the catalytic results showed that the yields in acetaldehyde and methyl formate are ten and four times higher, respectively, when the LHC is used. A Rh-containing species ($Rh_{1.32}Cr_{0.66}O_3$) has been used as co-catalyst in the CO_2 reduction into methanol, while the catalyst is a solid solution of Cu, Ag, In, Zn, and S [71]. However, the catalytic performances of such couple are lower than those when the Rh co-catalyst is replaced with RuO_2.

Recently, the very same rhodium-based electrocatalysts discovered by the end of the twentieth century (see Scheme 9) were reported to be active photocatalyst for the reduction of CO_2 into formic acid [72]. By careful engineering of the 2,2′-bipyridine moiety, it was possible to enchase this molecular Rh(III) arrange-ments in a solid crystalline scaffold, namely, metal-organic framework MOF UiO-67 (see Scheme 10). Interestingly, the catalytic behavior of Cp*Rh(bpydc) Cl_2 (bpydc = 2,2′-bipyridine-5,5′-dicarboxylic acid) in solution and supported in MOF UiO-67 is similar as demonstrated by the similar TON values (42 and 47 for
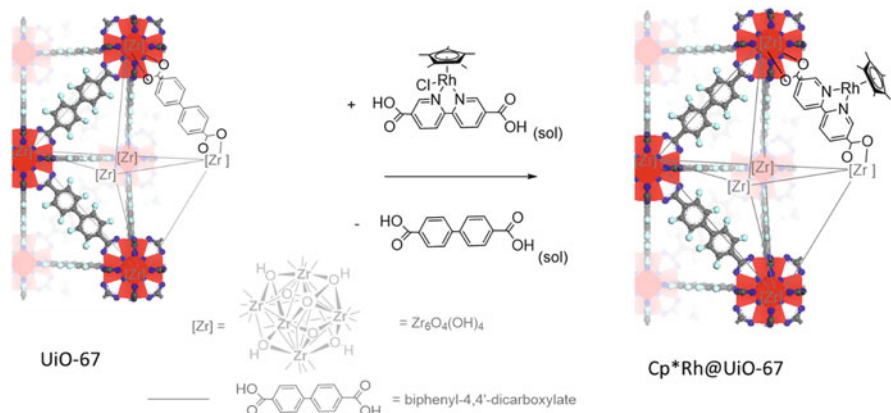
Scheme 10 UiO-67 functionalization with the active photocatalytic species: Cp*Rh(bpydc)Cl$_2$ [72]

the unsupported and for the MOF-supported, respectively) [72], thus providing an example of a Rh-based solid system en route to the artificial leaf objective [73].

5 Conclusion

In conclusion, rhodium has a very well-established track record as an early key player in the catalytic reduction of carbon dioxide. The first examples reported in molecular chemistry were almost concomitant with that of several Rh-based Wilkinson-type catalyst deployments which contributed to several major industrial milestones; rhodium was indeed a key element in the Monsanto process for acetic acid production, in the asymmetric hydrogenation in L-DOPA production and is still very present in the three-way catalytic converter for deNOx activity or in the asymmetric isomerization en route to menthol [32]. The activation of CO$_2$ was therefore one among of the several landmark achievements for this metal with many industrial applications.

As a member of the platinum group metals (PGM) cluster, rhodium also suffers from the same cost issues of its congeners. This aspect explains in part the subsequent research effort dedicated at its substitution by more accessible and possibly even more active alternative. Nevertheless, rhodium continues to play a key role, either because its content has been successfully diluted rather than fully removed (e.g., Ni–Rh systems) or because it is active in cutting edge applications where the frontier is more about finding some activity at all, rather than improving existing ones. Photocatalysis is a paragon of this strategy, since it aims at the blue sky objective of injecting REN in our current infrastructure. In this area, rhodium-based catalysts are among the key molecular species. This exemplifies well that rhodium is still front and center in many crucial field of catalysis, among which carbon dioxide utilization.

References

1. Lawrence Livermore National Laboratory. https://flowcharts.llnl.gov/content/assets/images/charts/Energy/ENERGY_2011_WORLD.png. Accessed 26 June 2016
2. International Energy Agency (2015) World Energy Outlook 2015
3. International Energy Agency. http://www.iea.org/publications/scenariosandprojections/. Accessed 29 June 2016
4. DePaolo DJ, Cole DR (2013) Geochemistry of geologic carbon sequestration: an overview. Rev Mineralogy Geochem 77(1):1–14
5. Aresta M, Dibenedetto A, Quaranta E (2016) J Catalysis. http://dx.doi.org/10.1016/j.jcat.2016.04.003
6. Liu Q, Wu L, Jackstell R, Beller M. Using carbon dioxide as a building block in organic synthesis
7. Styring P, Armstrong K, Quadrelli EA (eds) (2014) Carbon dioxide utilisation: closing the carbon cycle, 1st ed. Elsevier, Amsterdam, ISBN: 978-0-444-62746-9, 311 pp
8. Quadrelli EA, Centi G, Duplan J-L, Perathoner S (2011) Carbon dioxide recycling: emerging large-scale technologies with industrial potential. ChemSusChem 4(9):1194–1215
9. Centi G, Quadrelli EA, Perathoner S (2013) Catalysis for CO₂ conversion: a key technology for rapid introduction of renewable energy in the value chain of chemical industries. Energy Environ Sci 6(6):1711–1731
10. Klankermayer J, Leitner W (2016) Harnessing renewable energy with CO2 for the chemical value chain: challenges and opportunities for catalysis. Philos Trans A Math Phys Eng Sci 374 (2016)
11. Dechema Gesellschaft für Chemische Technik und Biotechnologie e. V International Energy Agency (IEA) and International Council of Chemical Associations (ICCA) Technology Roadmap. https://www.iea.org/publications/freepublications/publication/Chemical_Roadmap_2013_Final_WEB.pdf. Accessed 24 June
12. Hietala J, Vuori A, Johnsson P, Pollari I, Reutemann W, Kieczka H (2000) Formic acid. In: Ullmann's encyclopedia of industrial chemistry. Wiley-VCH Verlag GmbH & Co. KGaA
13. Joó F (2008) Breakthroughs in hydrogen storage—formic acid as a sustainable storage material for hydrogen. ChemSusChem 1(10):805–808
14. Loges B, Boddien A, Junge H, Beller M (2008) Controlled generation of hydrogen from formic acid amine adducts at room temperature and application in H2/O2 fuel cells. Angew Chem Int Ed 47(21):3962–3965
15. Fellay C, Dyson PJ, Laurenczy G (2008) A viable hydrogen-storage system based on selective formic acid decomposition with a ruthenium catalyst. Angew Chem Int Ed 47(21):3966–3968
16. Inoue Y, Izumida H, Sasaki Y, Hashimoto H (1976) Catalytic fixation of carbon dioxide to formic acid by transition-metal complexes under mild conditions. Chem Lett 5(8):863–864
17. Ezhova NN, Kolesnichenko NV, Bulygin AV, Slivinskii EV, Han S (2002) Hydrogenation of CO2 to formic acid in the presence of the Wilkinson complex. Russ Chem Bull 51 (12):2165–2169
18. Leitner W, Dinjus E, Gaßner F (1994) Activation of carbon dioxide. J Organomet Chem 475 (1):257–266
19. Fornika R, Gorls H, Seemann B, Leitner W (1995) Complexes [(P2)Rh(hfacac)] (P2 = bidentate chelating phosphane, hfacac = hexafluoroacetylacetonate) as catalysts for

CO2 hydrogenation: correlations between solid state structures, 103Rh NMR shifts and catalytic activities. J Chem Soc Chem Commun (14):1479–1481

20. Angermund K, Baumann W, Dinjus E, Fornika R, Görls H, Kessler M, Krüger C, Leitner W, Lutz F (1997) Complexes [(P2)Rh(hfacac)] as model compounds for the fragment [(P2)Rh] and as highly active catalysts for CO2 hydrogenation: the accessible molecular surface (AMS) model as an approach to quantifying the intrinsic steric properties of chelating ligands in homogeneous catalysis. Chem Eur J 3(5):755–764

21. Gassner F, Leitner W (1993) Hydrogenation of carbon dioxide to formic acid using water-soluble rhodium catalysts. J Chem Soc Chem Commun (19):1465–1466

22. Jessop PG, Joó F, Tai C-C (2004) Recent advances in the homogeneous hydrogenation of carbon dioxide. Coord Chem Rev 248(21–24):2425–2442

23. Musashi Y, Sakaki S (2002) Theoretical study of Rhodium(III)-catalyzed hydrogenation of carbon dioxide into formic acid. Significant differences in reactivity among Rhodium(III), Rhodium(I), and Ruthenium(II) complexes. J Am Chem Soc 124(25):7588–7603

24. Li Y-N, He L-N, Lang X-D, Liu X-F, Zhang S (2014) An integrated process of CO2 capture and in situ hydrogenation to formate using a tunable ethoxyl-functionalized amidine and Rh/bisphosphine system. RSC Adv 4(91):49995–50002

25. Sakakura T, Choi J-C, Yasuda H (2007) Transformation of carbon dioxide. Chem Rev 107 (6):2365–2387

26. Ukai K, Aoki M, Takaya J, Iwasawa N (2006) Rhodium(I)-catalyzed carboxylation of aryl- and alkenylboronic esters with CO2. J Am Chem Soc 128(27):8706–8707

27. Mizuno H, Takaya J, Iwasawa N (2011) Rhodium(I)-catalyzed direct carboxylation of arenes with CO2 via chelation-assisted C–H bond activation. J Am Chem Soc 133(5):1251–1253

28. Suga T, Mizuno H, Takaya J, Iwasawa N (2014) Direct carboxylation of simple arenes with CO2 through a rhodium-catalyzed C–H bond activation. Chem Commun 50(92):14360–14363

29. Kawashima S, Aikawa K, Mikami K (2016) Rhodium-catalyzed hydrocarboxylation of olefins with carbon dioxide. Eur J Org Chem

30. Ostapowicz TG, Schmitz M, Krystof M, Klankermayer J, Leitner W (2013) Carbon dioxide as a C1 building block for the formation of carboxylic acids by formal catalytic hydrocarboxylation. Angew Chem Int Ed 52(46):12119–12123

31. Maitlis PM, Haynes A, Sunley GJ, Howard MJ (1996) Methanol carbonylation revisited: thirty years on. J Chem Soc Dalton Trans (11):2187–2196

32. Gian Paolo Chiusoli PMM (2006) Metal-catalysis in industrial organic processes

33. Qian Q, Zhang J, Cui M, Han B (2016) Synthesis of acetic acid via methanol hydrocarboxylation with CO2 and H2. Nat Commun 7

34. Wu L, Liu Q, Jackstell R, Beller M (2014) Carbonylations of alkenes with CO surrogates. Angew Chem Int Ed 53(25):6310–6320

35. Aziz MAA, Jalil AA, Triwahyono S, Ahmad A (2015) CO2 methanation over heterogeneous catalysts: recent progress and future prospects. Green Chem 17(5):2647–2663

36. Wei W, Jinlong G (2011) Methanation of carbon dioxide: an overview. Front Chem Sci Eng 5 (1):2–10

37. Solymosi F, Erdöhelyi A, Bánsági T (1981) Methanation of CO2 on supported rhodium catalyst. J Catal 68(2):371–382

38. Ruiz P, Jacquemin M, Blangenois N (2010) Catalytic CO2 methanation process. Google Patents

39. Beuls A, Swalus C, Jacquemin M, Heyen G, Karelovic A, Ruiz P (2012) Methanation of CO2: further insight into the mechanism over Rh/γ-Al2O3 catalyst. Appl Catal B Environ 113–114:2–10

40. Karelovic A, Ruiz P (2013) Mechanistic study of low temperature CO2 methanation over Rh/TiO2 catalysts. J Catal 301:141–153

41. Jacquemin M, Beuls A, Ruiz P (2010) Catalytic production of methane from CO2 and H2 at low temperature: insight on the reaction mechanism. Catal Today 157(1–4):462–466

42. Karelovic A, Ruiz P (2012) CO2 hydrogenation at low temperature over Rh/γ-Al2O3 catalysts: effect of the metal particle size on catalytic performances and reaction mechanism. Appl Catal Environ 113–114:237–249
43. Ichikawa S (1995) Chemical conversion of carbon dioxide by catalytic hydrogenation and room temperature photoelectrocatalysis. Energy Conversion Manag 36(6–9):613–616
44. Karelovic A, Ruiz P (2013) Improving the hydrogenation function of Pd/γ-Al2O3 catalyst by Rh/γ-Al2O3 addition in CO2 methanation at low temperature. ACS Catal 3(12):2799–2812
45. Swalus C, Jacquemin M, Poleunis C, Bertrand P, Ruiz P (2012) CO2 methanation on Rh/γ-Al2O3 catalyst at low temperature: "In situ" supply of hydrogen by Ni/activated carbon catalyst. Appl Catal Environ 125:41–50
46. Aziz MAA, Jalil AA, Triwahyono S, Sidik SM (2014) Methanation of carbon dioxide on metal-promoted mesostructured silica nanoparticles. Appl Catal Gen 486:115–122
47. Zhang Y, Zhan X, Zheng X, Wang Z, Fang Z, Xue Y, Tao L (2015) Liquid catalyst for methanation of carbon dioxide. US 20150126626
48. Pakhare D, Spivey J (2014) A review of dry (CO2) reforming of methane over noble metal catalysts. Chem Soc Rev 43(22):7813–7837
49. Havran V, Duduković MP, Lo CS (2011) Conversion of methane and carbon dioxide to higher value products. Ind Eng Chem Res 50(12):7089–7100
50. Richardson JT, Paripatyadar SA (1990) Carbon dioxide reforming of methane with supported rhodium. Appl Catal 61(1):293–309
51. Zhang ZL, Tsipouriari VA, Efstathiou AM, Verykios XE (1996) Reforming of methane with carbon dioxide to synthesis gas over supported rhodium catalysts: I. Effects of support and metal crystallite size on reaction activity and deactivation characteristics. J Catal 158(1):51–63
52. Wang HY, Ruckenstein E (2000) Carbon dioxide reforming of methane to synthesis gas over supported rhodium catalysts: the effect of support. Appl Catal A Gen 204(1):143–152
53. Asencios YJO, Assaf EM (2013) Combination of dry reforming and partial oxidation of methane on NiO–MgO–ZrO2 catalyst: effect of nickel content. Fuel Process Technol 106:247–252
54. Jóźwiak WK, Nowosielska M, Rynkowski J (2005) Reforming of methane with carbon dioxide over supported bimetallic catalysts containing Ni and noble metal: I. Characterization and activity of SiO2 supported Ni–Rh catalysts. Appl Catal Gen 280(2):233–244
55. Estephane J, Ayoub M, Safieh K, Kaydouh M-N, Casale S, Zakhem HE (2015) CO2 reforming of CH4 over highly active and stable yRhNix/NaY catalysts. Comptes Rendus Chimie 18 (3):277–282
56. Basile F, Fornasari G, Poluzzi E, Vaccari A (1998) Catalytic partial oxidation and CO2-reforming on Rh- and Ni-based catalysts obtained from hydrotalcite-type precursors. Appl Clay Sci 13(5–6):329–345
57. Pakhare D, Wu H, Narendra S, Abdelsayed V, Haynes D, Shekhawat D, Berry D, Spivey J (2013) Characterization and activity study of the Rh-substituted pyrochlores for CO2 (dry) reforming of CH4. Appl Petrochem Res 3(3–4):117–129
58. Kusama H, Okabe K, Sayama K, Arakawa H (1996) CO2 hydrogenation to ethanol over promoted Rh/SiO2 catalysts. Catal Today 28(3):261–266
59. Kusama H, Okabe K, Sayama K, Arakawa H (1997) Ethanol synthesis by catalytic hydrogenation of CO2 over Rh-Fe/SiO2 catalysts. Energy 22(2–3):343–348
60. Ikehara N, Hara K, Satsuma A, Hattori T, Murakami Y (1994) Unique temperature dependence of acetic acid formation in CO2 hydrogenation on Ag-promoted Rh/SiO2 catalyst. Chem Lett 23(2):263–264
61. Ding Y-H, Huang W, Wang Y-G (2007) Direct synthesis of acetic acid from CH4 and CO2 by a step-wise route over Pd/SiO2 and Rh/SiO2 catalysts. Fuel Process Technol 88(4):319–324
62. Quadrelli EA (2016) 25 years of energy and green chemistry: saving, storing, distributing and using energy responsibly. Green Chem 18(2):328–330
63. Bolinger CM, Story N, Sullivan BP, Meyer TJ (1988) Electrocatalytic reduction of carbon dioxide by 2,2′-bipyridine complexes of rhodium and iridium. Inorg Chem 27(25):4582–4587

64. Caix C, Chardon-Noblat S, Deronzier A (1997) Electrocatalytic reduction of CO2 into formate with [(η5-Me5C5)M(L)Cl] + complexes (L = 2,2′-bipyridine ligands; M = Rh(III) and Ir(III)). J Electroanal Chem 434(1–2):163–170

65. Kushi Y, Nagao H, Nishioka T, Isobe K, Tanaka K (1994) Oxalate formation in electrochemical CO2 reduction catalyzed by rhodium-sulfur cluster. Chem Lett 23(11):2175–2178

66. Rasko J, Solymosi F (1994) Infrared spectroscopic study of the photoinduced activation of CO2 on TiO2 and Rh/TiO2 catalysts. J Phys Chem 98(29):7147–7152

67. Solymosi F, Tombácz I (1994) Photocatalytic reaction of H2O + CO2 over pure and doped Rh/TiO2. Catal Lett 27(1):61–65

68. Kohno Y, Hayashi H, Takenaka S, Tanaka T, Funabiki T, Yoshida S (1999) Photo-enhanced reduction of carbon dioxide with hydrogen over Rh/TiO2. J Photochem Photobiol A Chem 126 (1–3):117–123

69. Kohno Y, Yamamoto T, Tanaka T, Funabiki T (2001) Photoenhanced reduction of CO2 by H2 over Rh/TiO2: characterization of supported Rh species by means of infrared and X-ray absorption spectroscopy. J Mol Catal A Chem 175(1–2):173–178

70. Lee C-W, Antoniou Kourounioti R, Wu JCS, Murchie E, Maroto-Valer M, Jensen OE, Huang C-W, Ruban A (2014) Photocatalytic conversion of CO2 to hydrocarbons by light-harvesting complex assisted Rh-doped TiO2 photocatalyst. J CO2 Utilization 5:33–40

71. Liu J-Y, Garg B, Ling Y-C (2011) CuxAgyInzZnkSm solid solutions customized with RuO2 or Rh1.32Cr0.66O3 co-catalyst display visible light-driven catalytic activity for CO2 reduction to CH3OH. Green Chem 13(8):2029–2031

72. Chambers MB, Wang X, Elgrishi N, Hendon CH, Walsh A, Bonnefoy J, Canivet J, Quadrelli EA, Farrusseng D, Mellot-Draznieks C, Fontecave M (2015) Photocatalytic carbon dioxide reduction with rhodium-based catalysts in solution and heterogenized within metal-organic frameworks. ChemSusChem 8(4):603–608

73. Centi G, Perathoner S (2000) Artificial leaves. In: Kirk-Othmer encyclopedia of chemical technology. Wiley